Computational Electromagnetic Analysis of Plasmonic Effects in Interdigital Photodetectors

Avery M. Hill[a,b], Ahmad I. Nusir[c], Paul V. Nguyen[a,c], Omar M. Manasreh[c], Joseph B. Herzog [a,d,e,*]

[a]Department of Physics, University of Arkansas, Fayetteville, AR, 72701, USA;
[b]Department of Mechanical Engineering, University of Arkansas, Fayetteville, AR, 72701, USA;
[c]Department of Electrical Engineering, University of Arkansas, Fayetteville, AR, 72701, USA;
[d]Microelectronics-Photonics Program, University of Arkansas, Fayetteville, AR, 72701, USA;
[e]Institute for Nanoscience and Engineering, University of Arkansas, Fayetteville, AR 72701, USA

ABSTRACT

Plasmonic nanostructures have been shown to act as optical antennas that enhance optical devices. This study focuses on computational electromagnetic (CEM) analysis of GaAs photodetectors with gold interdigital electrodes. Experiments have shown that the photoresponse of the devices depend greatly on the electrode spacing and the polarization of the incident light. Smaller electrode spacing and transverse polarization give rise to a larger photoresponse. This computational study will simulate the optical properties of these devices to determine what plasmonic properties and optical enhancement these devices may have.

The models will be solving Maxwell's equations with a finite element method (FEM) algorithm provided by the software COMSOL Multiphysics 4.4. The preliminary results gathered from the simulations follow the same trends that were seen in the experimental data collected, that the spectral response increases when the electrode spacing decreases. Also the simulations show that incident light with the electric field polarized transversely across the electrodes produced a larger photocurrent as compared with longitudinal polarization. This dependency is similar to other plasmonic devices. The simulation results compare well with the experimental data. This work also will model enhancement effects in nanostructure devices with dimensions that are smaller than the current samples to lead the way for future nanoscale devices. By seeing the potential effects that the decreased spacing could have, it opens the door to a new set of devices on a smaller scale, potentially ones with a higher level of enhancement for these devices.

In addition, the precise modeling and understanding of the effects of the parameters provides avenues to optimize the enhancement of these structures making more efficient photodetectors. Similar structures could also potentially be used for enhanced photovoltaics as well.

Keywords: Computational electromagnetics, nanostructure, photovoltaics, simulation, photodetectors, plasmons, plasmonics, and modeling

1. INTRODUCTION

Computational electromagnetics (CEM) employs computer algorithms to provide solutions to complex electromagnetic problems; two popular methods in CEM are finite-difference time domain (FDTD) and finite-element method (FEM). The FDTD method employs a time domain to solve time dependent Maxwell's equations in partial differential equation form.[1] This study, however, will use COMSOL 4.4 software, which employs a FEM by breaking the space into a finite quantity of elements. This discretization of elements allows for these electromagnetic waves represented by complex differential equations to be expressed as basic functions.[2] This component of FEM allows for very complex electromagnetic equations to be summarized in such a way that is not computationally intensive when compared to the number of elements that are created when finding a solution.

The purpose of this CEM study is to analyze and further understand the potential plasmonic effects that could be occurring in an interdigital photodetector that is larger than customary devices that exhibit plasmonic activity; and to

* Email: jbherzog@uark.edu

Plasmonics: Metallic Nanostructures and Their Optical Properties XII, edited by Allan D. Boardman, Proc. of SPIE Vol. 9163, 91633Q · © 2014 SPIE
CCC code: 0277-786X/14/$18 · doi: 10.1117/12.2074251

investigate the plasmonic enhancement that would occur if one were to fabricate these devices with geometrical specifications at the nanoscale.

Plasmons are collective charge density oscillations of electrons that typically occur on metallic surfaces, and plasmonics is the study of these oscillations of electrons. This paper will focus on the plasmonic effects occurring for both micro and nanoscale devices composed of an Au electrode, a Ti adhesion layer, and a GaAs semiconductor substrate. Similar microelectronic and photonic devices have been fabricated and discussed in a previous work.[3]

With the expansion of nanotechnology and the vastly improving computing power available currently, CEM has been explored in new and exciting mediums. Solutions to these complex electromagnetic problems are now available at the command of a few keystrokes, with the new level of computational ability, device optimization and creation is now more possible for device manufacture. CEM brings theoretical results that will help tune devices and systems for improved spectroscopies[4], single molecule detection[4], and higher efficiency photovoltaics[5].

2. DEVICE DETAILS AND SIMULATION SETUP

Semi-insulating GaAs photodetectors have been fabricated with interdigital gold electrode similar to the CdSe nanocrystal devices in previous work[3]. The electrode design of the devices is shown in Figure 1. They are gold electrodes with a titanium adhesion layer. Devices with various electrode widths, *w*, and electrode spacing, *d*, were fabricated; and the ratio between the width of the electrode and the electrode spacing was kept constant so that $w = 2d$, as the spacing increased for various device sizes.

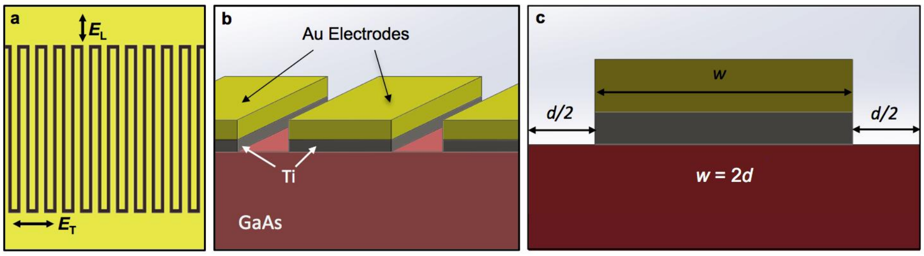

Figure 1. Interdigital photodetector design. (a) Schematic of device overview with transverse, E_T, and longitudinal, E_L, polarizations labeled (b) Cross-section of photodetector device, with electrodes made of Au with a Ti adhesion layer of width *w*, attached to a semi-insulating GaAs substrate. (c) Simulation space used for the finite element method (FEM) analysis. Devices are designed with the ratio of $w = 2d$, where *d* is the electrode spacing. The device is centered at the origin of the simulation space, with $d/2$ on either side. Left and right sides of the simulation space have periodic boundary conditions.

For this work, the devices were simulated with a two-dimensional cross-section model. In COMSOL, two-dimensional simulations are treated as if they are infinitely long in the z-direction. For these particular device simulations, the top and bottom boundaries of the simulation space of Figure 1c were designated as perfectly matched layers (PMLs). This ensured that once the applied electromagnetic waves were transmitted or reflected from the device, they were themselves absorbed so that they did not reflect back into the system and induce noise in the system. PML boundaries act as infinite boundaries in the directions they have been placed[1,2]. The two boundaries to the left and right of the device are not PMLs; instead they have been defined as periodic boundaries to simulate the periodicity of this device as shown by Figure 1a. The electrode had been centered at the origin of the simulation space with a distance of $d/2$ on either side. The entire simulation space (and the period of the device) has a width of $1.5w$, with *w* corresponding to the width of the electrode. The ratio between the width of the electrodes and the distance separating each electrode has been kept constant, $w = 2d$, to be consistent with the geometry of the fabricated devices. The material properties for GaAs, Ti, and Au were added to the model to accurately represent the device structure.

This work created a model using the radio frequency (RF) module of COMSOL 4.4 to analyze these devices. This model is robust and has the capability to simulate variable physical parameters of the system in order to determine the enhancements properties of these devices. Variable input parameters include particular polarization, directional poynting vectors, material parameters, and geometry. The wave equation to simulate these desired mechanics is $E_{b,X} = e^{ik_0 y}$; this equation represents the background electric field that was incident on the structure for all simulations where a perfectly transverse polarization was employed. The equation components are as follows, *i* representing a complex number, k_0

representing the initial wave number, and y is the poynting vector direction, the direction in which light is propagating for this simulation. For this study, a perfectly transverse wave has been defined as a wave with polarization completely in the x-direction, and a perfectly longitudinal wave as a wave with polarization completely in the z-direction. For the longitudinal wave equation the background field would be $E_{b,Z}$.

3. POLARIZATION STUDY OF MICRODEVICES

The polarization dependence exhibited by the devices was analyzed with this model. Experimental results have shown some polarization dependence with transverse polarization giving larger photo-response in the photodetectors. Therefore, this model measures this polarization dependence and computes the local electric field distribution near the nanoscale edge of the electrodes. In order to change the induced polarization within the simulation, the background electric field component was changed. Rather than the defining the background electric field in the x-direction as previously shown, this analysis will also take into account the following equation: $E_{b,Z} = e^{ik_0 y}$. All of the components of the wave equation are still intact, the only change being the direction in which the light is polarized, namely longitudinally (in the z-direction).

Figure 2 shows the results of computational simulations for both perfectly transverse (a) and longitudinal (b) polarizations of a device of electrode spacing, d = 5 µm. The color scale is plotting the electric field distribution, which is a unitless value defined as E_{local}/E_0, and the maximum value of the E-field distribution was 1.866 for the transverse polarization making the total enhancement factor equal to 3.48. The images only show the section of the model near the electrode edge, at the interface between the electrode and the space between the electrodes. For most plasmonic devices, the gaps between structures are where the most optical enhancement occurs[4,6]. This is also shown by the theoretical results as well, as the distance from the electrode end increased, the E-field distribution drastically decreased.

As shown by the two images, the transverse polarization Figure 2a had a span of color from a light blue to dark red, with red representing the largest electric field; whereas, the longitudinal polarization (Figure 2b) had almost no change in color intensity and is mostly blue, the weakest electric field distribution. The transverse polarization also shows a collection of hotspots that are likely due to plasmons oscillating on the edge-surface of the electrode. The hot spots are located at the top corner, at the intersection of the Au and Ti adhesion layer, and at the intersection of the Ti adhesion layer and the GaAs substrate.

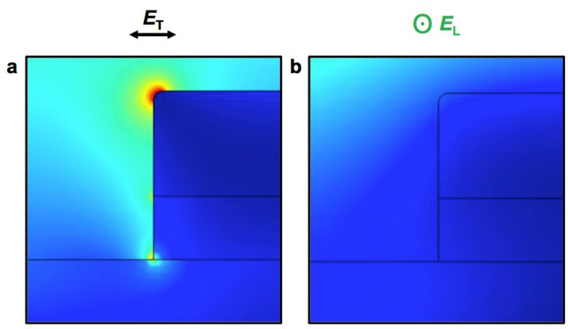

Figure 2. COMSOL simulation images of electric field distribution for a device with 5 µm electrode spacing, with a wavelength of 875 nm for (a) transverse, E_T, and (b) longitudinal, E_L, incident light polarization directions.

The total enhancement factor, G, of these devices is determined by equation (1),

$$G = \left|\frac{E_{local}^2}{E_0^2}\right|, \tag{1}$$

where the local electric field is computed during the simulation near the structure, and the initial electric field, $E_0 = E_b$ = 1 V/m. Therefore, the total enhancement of the device is the electric field distribution shown in Figure 2 squared, and the enhancement changes as a function of position along the structure. One of the strong hotspots extends into the GaAs substrate. Therefore, more electrons can be generated, and the plasmonic properties of the structure edge can enhance the photoresponse. These results can explain why the transverse polarization gives stronger photo-response for these devices than the longitudinal incident light.

4. THEORETICAL ANALYSIS OF NANOSTRUCTURES

Presently only microscale photodetectors have been fabricated. This work also examined nanostructure models for potential nanofabrication of similar structures. Much of this was to understand what would occur with the device at this scale and determine how the material components, geometrical ratios, and intrinsic properties of the materials would be affected when the device scaled to nanometers.

Due to a polarization dependence being discovered for the larger devices, these simulations focused only on a perfectly transverse polarization and at a specified wavelength of 875 nm. The simulation space was set up in such a way that preserved the relationship between the distance separating electrodes and the electrode width, keeping the $w = 2d$ relationship. A parametric sweep was employed so that the process could be automated; the width of electrode began at 50 nm and progressed to 1000 nm with a 1 nm step-size. Figure 3e plots the enhancement factor in the gap between the electrodes for each device of these various widths and also for a device of w = 10,000 nm (an electrode spacing, d, of 5 µm). This additional device size was included to show that the enhancement for devices is nearly constant as the device size increases, with $E^2_{local} / E^2_0 \cong 3.8$, and because theoretical enhancement values for a device of this size were gathered in previous trials, as shown in Figure 2.

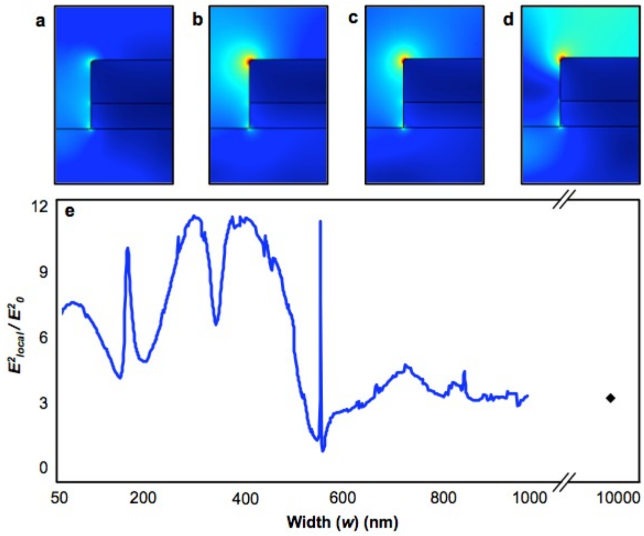

Figure 3 – FEM analysis of nanodevices of varying width, (a-d) COMSOL electric field distributions for device widths of (a) 184 nm, (b) 328 nm, (c) 424 nm, and (d) 576 nm. These figures do not show the entire simulations space. Instead they only show the area near the edge of the electrode. (e) The optical enhancement as a function of device width for a nanostructure with incident light at a constant wavelength of 875 nm and transverse polarization. The black diamond plots the electric field for a device of 10000 nm width.

The electric field distribution images, Figure 3a-d, show the electrical response for the devices with the greatest enhancement along the electrode edge, these device sizes theoretically provided the greatest optical enhancement. Each of the images showed hotspots congregated at roughly the same locations at the electrode edge. The device width that exhibits the greatest overall optical gain was 576 nm. This is likely due to the periodicity of the device electrodes (and the simulation space) patterning that has been defined and exhibited potential plasmonic grating effects[7,8]. The entire width of the simulation space is equal to the period of the electrode grating. For this device the width was 864 nm, which is almost equal to the wavelength of light being simulated, 875 nm.

5. CONCLUSION AND FUTURE WORK

This work, which focused on investigating the potential plasmonic activity occurring in microelectronic and photonic devices, also studied the effects of the same properties at the nanoscale. With the polarization dependence exhibited by the microdevice, it leads to the conclusion that there is likely some plasmonic activity occurring at the edge of the structure, even with the large geometrical area of the electrode. The same model is exhibited at the nanoscale, with this work only concerned with perfectly transverse or longitudinal polarizations, variable polarization angle should be examined in future works. Also, when the photodetector is simulated at the nanoscale, there is a dependence of enhancement factor to the width of the structure but with the added component of a correlation between periodicity of the structure and optical gain. More work is needed to fully decipher the effects of periodicity of the device and to analyze the effects of a variable polarization angle, electrode spacing.

CEM allows for complex geometrical, material, and physical properties to be simulated and examined with greater precision that previously allowed. These simulations will provide vast amounts of information to better fabricate and design these photodetector devices, and through simulation work, the devices can be tuned to specific applications and desired optical enhancements.

ACKNOWLEDGEMENTS

This work was partially supported by the Air Force Office of Scientific Research (Grantno.FA9550-10-1-0136), the NSF-EPSCOR Program (Grantno.EPS-1003970), and NASA (Grantno.242026- 1BBX11AQ36A). AMH would like to acknowledge the Honors College at the University of Arkansas for funding his research through the Honors College Research Grant 2014 and the Honors College Travel Grant; he would also like to thank SPIE for travel grant support. JBH would like to thank the Department of Physics, the Fulbright College of Arts and Science, and the Vice Provost for Research and Economic Development at the University of Arkansas for providing research funding, and for the Honors College Mentor Award fund at the University of Arkansas. Additionally, AMH and JBH would like to thank Ken Vickers and the MicroEP program for COMSOL license support.

REFERENCES

[1] Deinega, A., Belousov, S.., Valuev, I., "Hybrid transfer-matrix FDTD method for layered periodic structures," Opt. Lett. **34**(6), 860–862 (2009).

[2] E. Vandenbosch, G. A., "Computational Electromagnetics in Plasmonics," [Plasmonics - Principles and Applications], K. Y. Kim, Ed., InTech (2012).

[3] Nusir, A. I., Aguilar, J., Bever, Z.., Manasreh, M. O., "Uncooled photodetectors based on CdSe nanocrystals with an interdigital metallization," Appl. Phys. Lett. **104**(5), 051124 (2014).

[4] Herzog, J. B., Knight, M. W., Li, Y., Evans, K. M., Halas, N. J.., Natelson, D., "Dark Plasmons in Hot Spot Generation and Polarization in Interelectrode Nanoscale Junctions," Nano Lett. **13**(3), 1359–1364 (2013).

[5] Atwater, H. A.., Polman, A., "Plasmonics for improved photovoltaic devices," Nat. Mater. **9**(3), 205–213 (2010).

[6] Natelson, D., Li, Y.., Herzog, J. B., "Nanogap structures: combining enhanced Raman spectroscopy and electronic transport," Phys. Chem. Chem. Phys. **15**(15), 5262 (2013).

[7] Todorov, Y., Tosetto, L., Teissier, J., Andrews, A. M., Klang, P., Colombelli, R., Sagnes, I., Strasser, G.., Sirtori, C., "Optical properties of metal-dielectric-metal microcavities in the THz frequency range," Opt. Express **18**(13), 13886–13907 (2010).

[8] Steele, J., Moran, C., Lee, A., Aguirre, C.., Halas, N., "Metallodielectric gratings with subwavelength slots: Optical properties," Phys. Rev. B **68**(20) (2003).